Characteristics of Refrigerant Flow through Capillary Tubes and Short Tube Orifices

Yongchan Kim* and Jongmin Choi**

Key Words: Capillary Tube, Short Tube Orifice, Expansion Device, Flow Control

Abstract

The capillary tube and short tube orifice have been widely used as an expansion device in the refrigeration and air-conditioning system. To improve the system performance, expansion devices need to be optimized with the components of a refrigeration system. In the present study, a numerical model for a capillary, which could predict the flow rate and properties along a tube, was developed by assuming homogeneous two-phase flow. A semi-empirical flow model for evaluation of the flow rate through a short tube orifice was also developed by using the experimental data. Finally, the results of the numerical model for a capillary was compared with those of the semi-empirical model for a short tube orifice to identify the dominant flow factors for the expansion devices.

Nomenclature

A_s : capillary/short tube cross-sectional area [㎡]
C_{tp} : correction factor for two-phase flow
D : capillary/short tube diameter [mm]
DR : D / D_{ref}
D_{ref} : reference short tube diameter [1.524mm]
$EVAP$: normalized downstream pressure
f : friction factor
G : mass flux [kg/(h · ㎡)]
h : enthalpy [kJ/kg]
k : Boltzmann constant
L : capillary/orifice length [mm]
$\dot{m}$: mass flow rate [kg/h]
P : pressure [kPa]
P_{down} : downstream pressure [kPa]
P_f : adjusted downstream pressure [kPa]
PRA : P_{up} / P_c
P_{up} : upstream pressure [kPa]
P_v : evaporating pressure [kPa]

* Department of Mechanical Engineering, Korea Univ. Seoul, Korea
** Graduate School, Korea Univ., Seoul, Korea

SUB : $(T_{sat} - T_{up}) / T_c$
T : temperature [C, K]
ΔT_{SC} : subcooling [℃]

Greek symbols

χ : quality
ν : specific volume [m³/kg]
z : axial length [mm]
ε : roughness [mm]
ρ : density [kg/m³]
τ_w : wall shear stress [kPa]
σ : surface tension [N/m]
μ : viscosity [Pa · s]

Subscripts

c : critical state
down : downstream
f : saturated liquid
g : saturated vapor
sat : saturation
tp : two-phase
up : upstream

1. Introduction

An expansion device which is an important component of the refrigeration system controls the mass flow rate and balances the system pressure. A capillary tube has been widely used in a refrigerator and small system, due to its high reliability and low cost. Short tube and TXV(thermostatic expansion valve) are mostly applied to heat pump and residential air conditioner. Usage of short tube orifice has been increased, because of its low cost, high reliability, ease of installation and inspection, and elimination of the additional check valves used for flow direction change in heat pump applications.

Most of previous work through the capillary tube and short tube orifice concentrated on CFC-12 and HCFC-22. A great deal of research and development is currently underway to identify the substitutes for HCFCs. Bolstads and Jordan[1] verified the critical flow in the capillary tube. Metastable flow in the capillary tube were found by Dudley[2]. Kuehl and Goldschmidt[3] developed a model for HCFC-22 flow through the capillary tubes based on homogeneous flow assumption for two-phase flow region. Kim et al.[4] established a numerical model considering the roughness to predict the capillary tube performance. Chang et al.[5] developed an empirical model to estimate the metastable flow in the capillary tube using HFC refrigerants.

Aaron and Domanski[6] developed a semImpirical flow model which could predict the mass flow rate in a short tube orifice, for subcooled condition at the inlet of short tube orifice. Using HFC refrigerants, Kim and O'Neal[7,8] made an empirical flow model to predict the performance of the short tube orifice for subcooled and two-phase conditions at the inlet of the short tube orifice.

In the present study, the mass flow rate and performance of capillary tube were analyzed using the numerical model for the capillary tube. The modeling results for the capillary tube were compared with those of the experiments for the short tube orifices. It is difficult to compare the characteristics of capillary tube with that of short tube orifice, because the operating ranges of those are not the same. Therefore, the qualitative analysis for the capillary tube and short tube orifice was performed with operating parameters.

2. Experimental apparatus and procedure

A schematic diagram of the experimental setup is shown in Fig.1. The test loop was designed to allow easy control of each operating parameters such as upstream subcooling, upstream pressure, and downstream pressure. The test rig consisted of a refrigerant flow loop containing a detachable test section, a hot water flow loop, and water/glycol flow loop. The liquid pump with a variable speed motor was used to control the wide refrigerant mass flow rate and upstream pressure. The refrigerant subcooling entering the test section was set by a water heated heat exchanger (evaporation heat exchanger) and a heat tape. The pressure and temperature at the exit of the test section was controlled by adjusting the temperature and flow rate of chilled water/glycol entering the heat exchanger. Fig.2(a) shows the schematic of the orifice test section for routine performance tests. The schematic of a short tube orifice used for pressure profile measurements is shown in Fig.2(b). Five pressure taps were located inside the short tube.

Performance tests were executed by varying the upstream pressure, downstream pressure, and inlet subcooling and quality. Upstream pressure was maintained at saturated pressure corresponding to condensing temperature of 38 ℃, 45 ℃, and 52 ℃, while downstream pressure was set at saturated pressure of 7 ℃. For the short tube orifice, the quality was varied from 0 % to 10 %.

Temperatures, pressures, flow rate, and power input were monitored in the test loop using a computer data acquisition system. Each sensor was calibrated to reduce experimental uncertainties and connected to a data logger. All temperature measurements were made using the copper constant thermocouples, and the accuracy of the temperature measurement was estimated at 0.3 ℃. Pressure transducers for high and low pre-

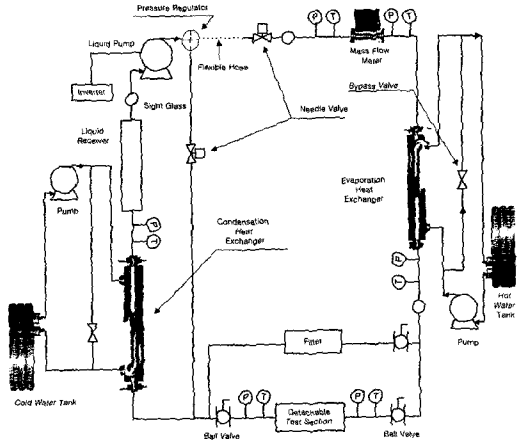

Fig.1 Schematic diagram of the experimental setup.

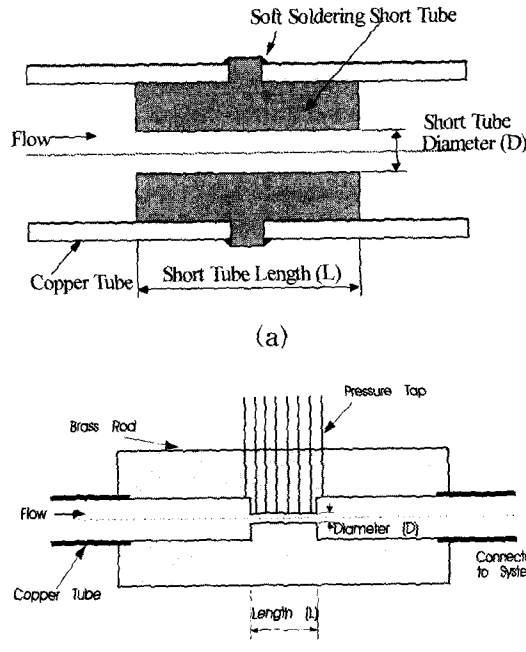

Fig.2 Test section of a short tube orifice.

ssure were used in measuring the refrigerant pressures. The estimated accuracy was 0.4 % of full scale (3447kPa) for high pressure transducers, and 0.2 % of full scale(1724 kPa) for low pressure transducers. The refrigerant flow rate was measured with a mass flow meter, and it was calibrated with water. The accuracy of the mass flow meter was 0.6 % of full scale (1.45GPM). Data were taken at steady state. The controlling parameters had to be within the following limits. : upstream pressure, 7 kPa; downstream pressure, 14 kPa; and subcooling, 0.3 ℃.

3. Numerical model for a capillary tube

The capillary tube has a simple structure, while it generates a complex flow field which includes sudden contraction, flashing, metastable flow, choking flow. In the present study, a numerical model of HCFC-22 flow through capillary tubes was developed at a steady state, adiabatic, and choked flow condition when downstream pressure was lower than saturated pressure according to inlet temperature. The model considered the metastable liquid flow using an empirical correlation. The effects of relative roughness inside tube was also included in this model.

3.1 Governing equation

Subcooled liquid region

The subcooled liquid region assumed to be incompressible flow. Pressure distribution of the liquid region was obtained from the equation of continuity and momentum.

$$dz = \frac{-dP}{fG^2/(2\rho_f D)} \tag{1}$$

Roughness() inside of the capillary tube was considered using the Colebrook equation which predicted the single-phase friction factor, f.

$$f = \frac{0.25}{[\log(\varepsilon/(3.7D) + 2.51/(Re\sqrt{f}))]^2} \tag{2}$$

Two-phase region

The pressure drop for the liquid region is linear, while for the two-phase region it is nonlinear. In the present study, two-phase flow as a function of the capillary tube length was calculated from the equations of energy and momentum for homogeneous two-phase flow (equation (3)).

$$\frac{dx}{dz} = -\frac{A}{B}\left(\frac{dP}{dz}\right)_{tp} \tag{3}$$

The pressure drop of the two-phase region was evaluated by adding the frictional and accelerational pressure drop(10).

$$-\left(\frac{dP}{dz}\right)_{tp} = \frac{-\left(\frac{dP}{dz}\right)_F + C\frac{dz}{dz}}{E} \tag{4}$$

$$A = x\frac{dh_g}{dP} + (1-x)\frac{dh_f}{dP} + G^2\nu_m\left[x\frac{d\nu_g}{dP} + (1-x)\frac{d\nu_f}{dP}\right]$$

$$B = h_{fg} + g^2\nu_m\nu_{fg}$$

$$C = G^2\nu_{fg}$$

$$E = 1 + G^2\left[x\frac{d\nu_g}{dP} + (1-x)\frac{d\nu_f}{dP}\right]\left(\frac{dP}{dz}\right)_F = -\frac{fG^2}{2D}\nu_m$$

Since equations (3) and (4) were coupled together, those were solved using the fourth order Runge-Kutta method. The two-phase friction factor was determined from Reynolds number and equation (2).

$$Re_{tp} = \frac{V_m D}{\mu_{tp}\nu_m} \tag{5}$$

The McAdams equation was applied for the

calculation of two-phase viscosity.

$$\frac{1}{\mu_{tp}} = \frac{x}{\mu_g} + \frac{(1-x)}{\mu_f} \tag{6}$$

Metastable flow region

It was noted that when subcooled liquid entered the capillary tube, the refrigerant was in a liquid state at the inlet section of the tube even though its pressure was lower than the saturation pressure. That was called the metastable flow. Actual evaporating pressure in a metastble state was calculated utilizing the Chen et. al's correlation(3).

$$\frac{(P_{sat}-P_v)\sqrt{kT_{sat}}}{\sigma^{3/2}} = 0.679\frac{\nu_g}{\nu_g-\nu_f}Re^{0.914} \times \left(\frac{\Delta T_{sc}}{T_c}\right)^{-0.208}\left(\frac{D}{D}\right)^{-3.18} \tag{7}$$

where, $D=\sqrt{kT_{sat}/\sigma}\times 10^4$,

3.2 Calculation procedure.

The model starts with the initialization of the mass flow rate and reading of the input data. The input required for this model are upstream pressure, subcooling or quality, downstream pressure and capillary tube geometry. The output from this model includes the mass flow rate, and variation of pressure, temperature inside of the tube.

Choking condition should be satisfied in the system with a constant area expansion device. This model assumed the choking condition at the exit of capillary tube, and the critical pressure was calculated using the Fanno curve. Pressure drops of single-phase and metastable region were calculated by equation (1), and that of two-phase region was modeled by equation (4). The convergence of the model was checked by comparing the assumed mass flow rate with the calculated.

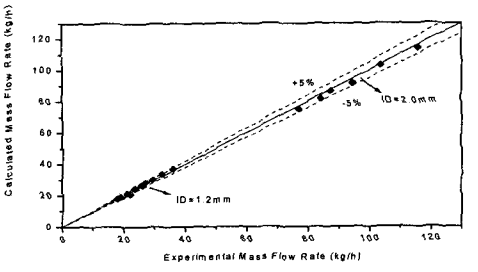

Fig.3 Comparison of experimental results with numerical results for capillary tubes.

Figure 3 shows the comparison of the experimental results with the numerical results for capillary tubes. The results of the model are consistent with the experimental data within 5%.

4. Mass flow model for a short tube orifice

4.1 Semi-empirical flow model

A mass flow model was developed to cover both single and two-phase flow at the inlet of the short tube orifice. Equation (8) represents the final semi-empirical model to predict the mass flow rate through a short tube orifice.

$$\dot{m} = c_{tp}\, A_s \sqrt{2g_c\rho(P_{up}-P_f)} \tag{8}$$

where, P_f is the adjusted downstream pressure before the flashing occurred, and Ctp is the two-phase correction factor for two-phase flow at the inlet of the short tube.

Correction factors, P_f and C_{tp} in equation (8) were correlated with respect to each operating parameters and short tube orifice geometry. After deciding basic normalized parameters included in each correction factor, a correlation

between the correction factor and the normalized parameters was determined using the nonlinear regression technique along with the experimental data. All coefficients included in this flow model are given in Table 1.

$$P_f = P_{sat}\left[\begin{array}{l} b_1 + b_2 \cdot PRA^{b_3} \cdot LD^{b_4} \cdot SUB^{b_5} \\ + b_6 \cdot PRA^{b_7} + b_8 \mathrm{EXP}\left(b_9 \cdot DR \cdot LD^{b_{10}}\right) \\ + b_{11} \cdot EVAP \end{array}\right] \quad (9)$$

$$C_{tp} = \frac{1}{\left(1 + a_{1x_{up}}\right) \cdot \left(1 + a_2 (LD)^{a_3} Y^{a_4 \mathrm{Ln}(LD)}\right)} \quad (10)$$

$$Y = \frac{x_{up}}{1 - x_{up}} \cdot \left(\frac{\rho_f}{\rho_g}\right)^{0.5} \quad (11)$$

where, $DR = D/D_{ref}$

$D = LD$

$EVAP = (P_c - P_{down})/P_c$

$PRA = P_{up}/P_c$

$SUB = (T_{sat} - T_{up})/T_c$

In equation (9), normalized parameters, PRA, SUB, DR, and EVAP were correlated with respect to upstream pressure, subcooling, diameter, and downstream pressure. For single-phase flow entering the short tube, C_{tp} was set to one.

4.2 Mass flow charts

To provide easier usage of a flow model, the flow charts were developed using the derived semi-empirical flow model for HCFC-22 (Equation (9)). The mass flow rate can be estimated using the equation (12) along with Figs. 4 ~ 6.

$$\dot{m} = \dot{m}_r \Phi_1 \Phi_2 \quad (12)$$

where, $\dot{m}_a$ is an actual mass flow rate. The reference short tube mass flow rate, $\dot{m}_r$, was

Table 1 Coefficients of correction factors in the flow model

Eq.	Coefficient	R-22
Eq. (9)	b_1	1.005
	b_2	5.737
	b_3	-0.485
	b_4	-0.179
	b_5	0.995
	b_6	0.268
	b_7	2.716
	b_8	-0.226
	b_9	-0.021
	b_{10}	2.000
	b_{11}	-0.092
	a_1	-5.870
	a_2	3.317
	a_3	0.231
	a_4	0.511

Constant	Unit	R-22
P_c	SI	4997.4 kPa
T_c	SI	369.17 K

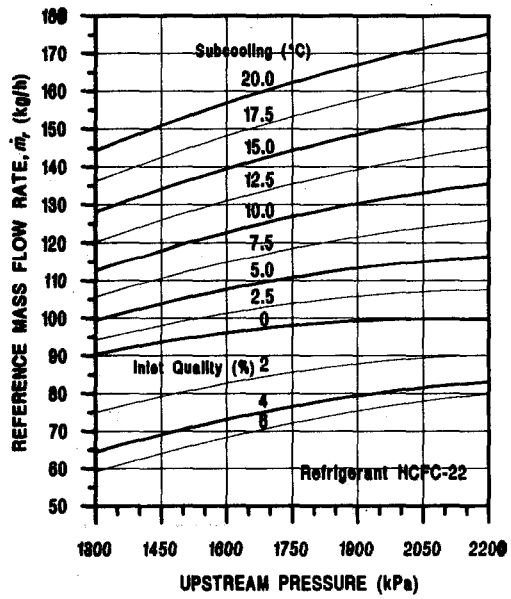

Fig.4 Reference mass flow rate for the standard short tube with L=12.70 mm, D=1.35 mm.

determined from Fig.4 with the given conditions for subcooling and upstream pressure. The effects of the geometry on the flow rate can be corrected using the correction factor, Φ_1, from Fig.5. Then, the subcooling correction factor, Φ_2, was obtained from Fig.6 to correct the effect of subcooling and L/D ratio. The reference short tube orifice was 12.7 mm length and 1.35 mm diameter.

5. Comparison of the flow characteristics of capillary tube with that of short tube orifice

The flow characteristics of capillary tube is similar to that of the short tube orifice, because they are constant area expansion devices. However, the pressure variation inside tube and the parameter affecting mass flow rate are different each other, because the length of a capillary tube is much longer than that of a short tube orifice. When subcooled liquid entered a capillary tube, flashing occurred inside of the tube. There was a large pressure drop just before the exit of the tube. While, for a short tube orifice, a large pressure drop was observed at the inlet region due to sudden contraction. The fluid is in the subcooled or metastable liquid state for the whole length of a short tube orifice.

When downstream pressure was lower than the saturation pressure corresponding to inlet temperature, the variation of mass flow rate was within 5% for capillary tubes or short tube orifices. From the present study it was observed that the non-ideal choking was occurred for the capillary tubes and short tube orifices. Choked flow has been defined as the phenomenon which occurred when the mass flow rate remained constant even when there was further reduction in downstream pressure.

Figures 7 and 8 show the pressure variation

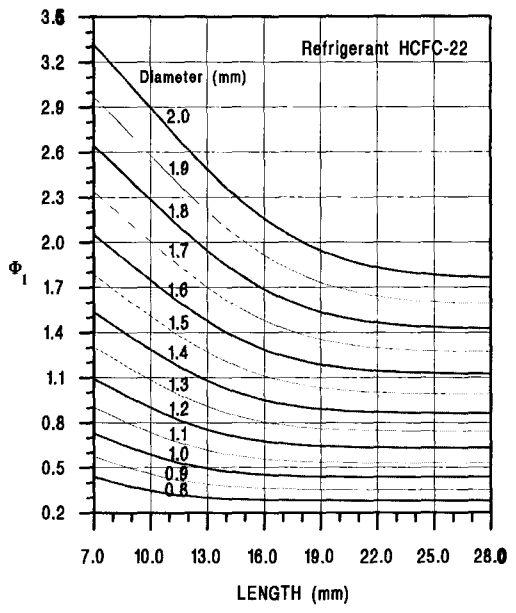

Fig.5 Correction factor for short tube geometry.

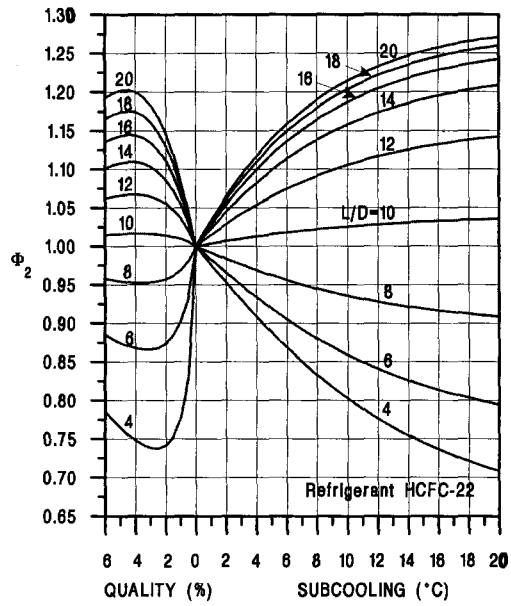

Fig.6 Correction factor for inlet subcooling or quality of short tube orifice.

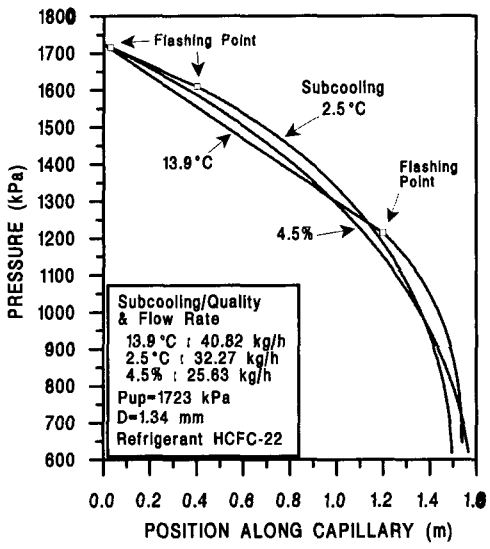

Fig.7 Pressure variation along the capillary tube.

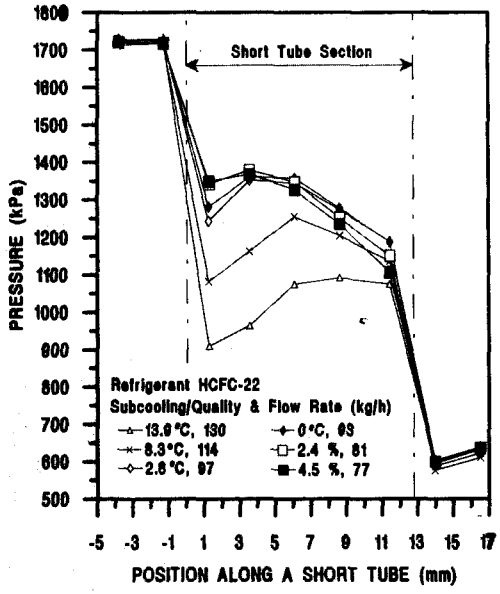

Fig.8 Pressure variation for the short tube with L=12.83mm and D=1.33mm.

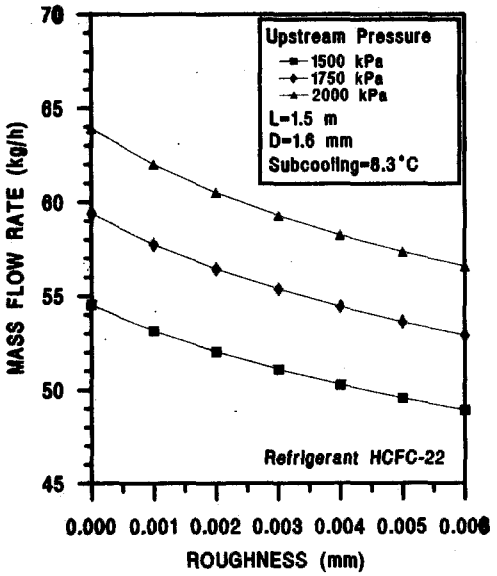

Fig.9 Flow dependency on roughness of a capillary tube.

for the capillary tube and the short tube orifice. Fig.7 was obtained from the numerical calculation, but Fig.8 was drawn using the experimental data. For a short tube orifice, a large pressure drop existed at the inlet of the tube. All of the pressure inside the tube increased as the subcooling decreased or as the quality increased. As the subcooling increased, the allowable subcooled pressure drop at the inlet of the short tube increased, thus the mass flow rate increased. For two-phase flow entering the orifice, the pressure at the inlet remained constant even though the quality increased. As the inlet quality increased, the mass flow rate decreased because of the increase in the void fraction at the entrance of the short tube.

For a capillary tube, pressure drop at the inlet of the tube was negligible. The mass flow rate depended on the pressure drop through the overall capillary tube length. When inlet subcooling was 13.9℃, flashing occurred at the point of 1.2 m from the inlet. As the subcooling decreased, mass flow rate and the slope of two-phase pressure drop decreased, and flashing point moved to the inlet. Theoretically, flashing

occurred at the saturation pressure. However, flashing was observed when the pressure was lower than the saturation pressure. It is called as delay of flashing. The mass flow rate increased with delay of flashing, due to a rise at the liquid region. Mass flow rate through a capillary tube was strongly dependent on the pressure drop inside the tube. The effect of roughness on a mass flow rate for a capillary tube was larger than that for a short tube orifice

Figure 9 shows the flow dependency on roughness of a capillary tube. As the roughness increased, the mass flow rate decreased. Fig.10 and 11 show the flow dependency on the upstream pressure for a capillary tube and short tube orifice respectively. Mass flow rate was directly proportional to the upstream pressure for both the capillary tube and the short tube orifice.

Figures 12 and 13 represent the mass flow rate dependency upon upstream subcooling or quality for a capillary tube and short tube orifice respectively. The flow trends of a capillary

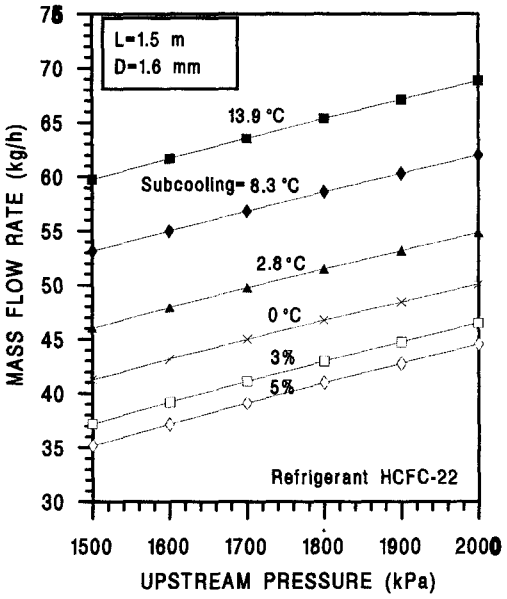

Fig.10 Flow dependency on upstream pressure for the capillary tube.

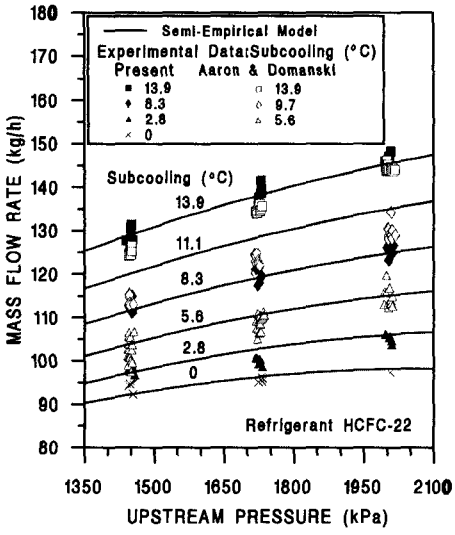

Fig.11 Flow dependency on upstream pressure for the standard short tube, L=12.70 mm and D=1.35 mm.

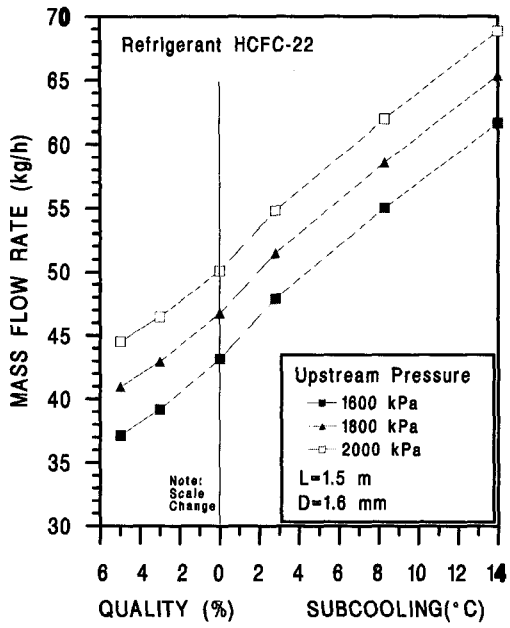

Fig.12 Flow dependency on upstream subcooling and quality for the capillary tube.

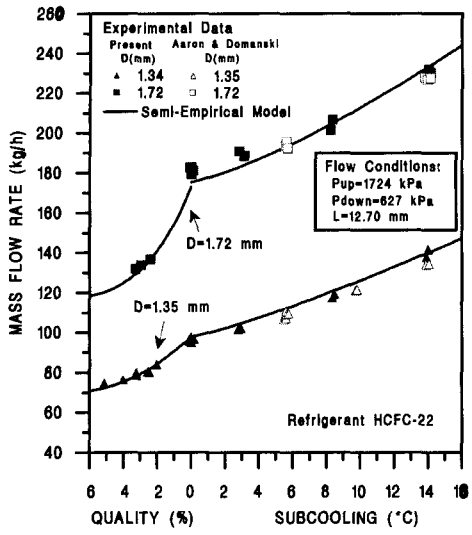

Fig.13 Flow dependency on upstream subcooling and quality for short tubes,

tube was similar to that of a short tube orifice. As the subcooling increased or the quality decreased, the mass flow rate increased. For a capillary tube, when subcooling increased, the flashing point moved to the exit and the density of the refrigerant increased. As a results, the mass flow rate increased. For a short tube orifice, as the quality rose, mass flow rate reduced because of the void fraction increase. When the quality increased, the reduction of mass flow rate for a short tube orifice was larger than that for a capillary tube.

6. Conclusions

In the present study, a numerical model for a capillary tube and a semi-empirical model for a short tube orifice were developed through the numerical analysis and the experimental study. The developed models allow to predict the flow characteristics and select the size of the constant area expansion devices. The following conclusions were derived from the present study.

(1) The flow at the exit of a capillary tube was in a equilibrium two-phase flow, while the flow of short tube orifice was in a metastable equilibrium all over the length because the tube length was too short.

(2) For a short tube orifice, when the subcooled liquid entered the expansion device, mass flow rate was governed by a pressure drop at the inlet region. When two-phase flow entered the short tube, it was determined by the void fraction and the pressure drop over the tube.

(3) For a capillary tube the inlet pressure drop was negligible, and the mass flow rate was dependent on internal pressure drop.

(4) Mass flow rate of the capillary tube and short tube orifice rely on the upstream pressure, subcooling or quality, and the geometry of the expansion device. While it was insensitive to a downstream pressure. As the upstream pressure and subcooling increased, mass flow rate was raised.

Acknowledgements

This work was supported by a grant, No 96-0200-12-03-3 from the Korea Science and Engineering Foundation.

Reference

(1) Bolstad, N.M., and R.C. Jordan., 1948, "Theory and Use of the Capillary Tube Expansion Device," *Refrigerating Engineering*, Vol. 56, No. 6, pp. 519-523.

(2) Dudley, J.K., 1962, *A Photographic Study of the Two-Phase Flow of Freon in Small Bore Tubes*, M.S. Thesis, Univ. of Wisconsin.

(3) Kuehl, S.J.,and Goldschmidt, V.W., 1991, "Modeling of Steady Flows of R-22 through Capillary Tube," *ASHRAE Trans.*, Vol. 97, Part 1, pp. 139-148.

(4) Kim, C.Y., Hwang, Y.P., Park, Y.M., 1995, "Investigation of the Performance of Capillary Tube with the Roughness Effect," *Proceeding of the SAREK Annual Summer Conference*, pp. 283-289.

(5) Chang, S.D., Ro, S.T., 1995, "Flow of Pure HFC Refrigerants and their Mixtures through a Capillary Tube," *Proceeding of the SAREK Annual Summer Conference*, pp. 263-268.

(6) Aaron, A.A, and Domanski, P.A.,1989, "An Experimental Investigating and Modeling of the Flow Rate of Refrigerant 22 through the Short Tube Restrictor," NISTIR-89-4120, US Department of Commerce.

(7) Kim, Y. and O'Neal D.L., 1994, "Two-Phase Flow of R-22 through Short Tube Orifices," *ASHRAE Trans.*, Vol. 100, Part 1, pp. 323-334.

(8) Kim, Y.C., 1996, "Experimentation and Modeling of R32/125/134a Flow through Short Tube Orifices," *J. of Air-Conditioning and Refrigeration*, Vol. 8, pp. 45-54.

(9) Gerhart, P.M., Gross, R., and Hochstein, J., 1992, *Fundamentals of Fluid Mechanics*, 2nd ed., Addison Wesley.

(10) Carey, V.P., 1992, *Liquid-Vapor Phase-Change Phenomena*, Taylor and Francis.

(11) Chen, Z., Li, R., Lin, S., Chen, Z.Y., 1990, "A Correlation for Metastable Flow of Refrigerant 12 through Capillary Tubes", *ASHRAE Trans.*, Vol. 96, Part 1, pp. 550-554.